Journal of Hazardous Materials 161 (2009) 933–940

Contents lists available at ScienceDirect

Journal of Hazardous Materials

journal homepage: www.elsevier.com/locate/jhazmat

Impregnated silica nanoparticles for the reactive removal of sulphur mustard from solutions

Beer Singh*, Amit Saxena, Anil Kumar Nigam, Kumaran Ganesan, Pratibha Pandey

PD Division, Defence R&D Establishment, Jhansi Road, Gwalior 474002, MP, India

ARTICLE INFO

Article history:
Received 25 January 2008
Received in revised form 11 April 2008
Accepted 11 April 2008
Available online 24 April 2008

Keywords:
Metal oxide nanoparticles
Impregnation
Adsorptive removal
Degradation
Bis-(2-chloroethyl)sulphide (sulphur mustard)

ABSTRACT

High surface area (887.3 m^2/g) silica nanoparticles were synthesized using aerogel route and thereafter, characterized by N_2-Brunauer–Emmet–Teller (BET), SEM and TEM techniques. The data indicated the formation of nanoparticles of silica in the size range of 24–75 nm with mesoporous characteristics. Later, these were impregnated with reactive chemicals such as *N*-chloro compounds, oxaziridines, polyoxometalates, etc., which have already been proven to be effective against sulphur mustard (HD). Thus, developed novel mesoporous reactive sorbents were tested for their self-decontaminating feature by conducting studies on kinetics of adsorptive removal of HD from solution. Trichloroisocyanuric acid impregnated silica nanoparticles (10%, w/w)-based system was found to be the best with least half-life value ($t_{1/2}$ = 2.8 min) among prepared systems to remove and detoxify HD into nontoxic degradation products. Hydrolysis, dehydrohalogenation and oxidation reactions were found to be the route of degradation of HD over prepared sorbents. The study also inferred that 10% loading of impregnants over high surface area and low density silica nanoparticles enhances the rate of reaction kinetics and seems to be useful in the field of heterogeneous reaction kinetics.

1. Introduction

In recent years, the scientific community has expressed increasing concern about the possibilities of use of toxic chemicals by terrorists and highly ambitious Nations. Thousand tons of these toxic chemical warfare (CW) agents exist with Nations having CW agent production capabilities. Spills of these toxic chemicals can create extreme environmental hazards, which must be effectively cleaned up and controlled. For that, investigations are underway to find safe and effective measures to detoxify these chemicals without endangering the human life or the environment. Moreover, the situation needs the development of suitable real-time decontamination materials, which can perform in situ degradation (physisorption followed by chemisorption) of CW agents. Highly porous multifunctional metal oxide nanoparticles have received enormous interest recently because of their unique physical and chemical properties [1]. These materials have been synthesized via soft chemistry by sol–gel processes and work as a destructive adsorbent due to its high surface area and chemical reactivity, i.e., initially the adsorbate molecules are physically adsorbed followed by dissociative chemisorption to such an extent that the chemical integrity of the adsorbate molecule is completely destroyed [1–3].

Koper and Klabunde [4] have discussed the use of metal oxide nanoparticles as destructive adsorbents for biological and chemical contamination. Her preferred metal oxides include MgO, CaO, TiO_2, ZrO_2, FeO, V_2O_3, Mn_2O_3, Fe_2O_3, NiO, CuO, Al_2O_3, ZnO, and their mixtures thereof; however, she has not used silica nanoparticles. Overall, as per literature high surface area metal oxide/hydroxide (except silica nanoparticles) nanoparticles having reactive surfaces have been used alone or mixed with decontamination solutions, foams, etc. for the degradation of CW agents [1–4]. As literature suggest that single metal oxide nanoparticles show promising results, but these nanoadsorbents can further be modified for second generation nanoadsorbents by loading/impregnation with those reactive compounds [5–10], which have already been proven to be active against CW agents. However, the possibility of use of new compounds for impregnation also does exist. Okun and Hill [11] have prepared the compositions of polyoxometalate/cationic silica material, copper salts and combinations thereof to decontaminate 2-chloroethylethyl sulphide (2-CEES). In addition to that, embodiments of decontaminating compositions comprising an inorganic nanoparticle and an organic reactive molecule (e.g.

* Corresponding author. Fax: +91 751 2341148.
E-mail addresses: beerbs5@rediffmail.com (B. Singh), amsa888@rediffmail.com (A. Saxena).

0304-3894/$ – see front matter © 2008 Elsevier B.V. All rights reserved.
doi:10.1016/j.jhazmat.2008.04.076

molecule with hydantoin rings) grafted via a linker group (polymer) on to the inorganic nanoparticle have also been discussed [12].

In addition to this, reactive chemicals such as *N*-chloro compounds [7,9,10], oxaziridines [8], etc. have been widely used for the decontamination of CW agents, but these have never been loaded on metal oxide nanoparticles especially silica to degrade CW agents. This attracts the attention to explore the opportunity. If reactive nanoparticles (alumina, magnesium or calcium oxide, etc.) have been impregnated with reactive chemicals, then the chances of cross-reaction do exist, this may destroy the reactivity of both. Therefore, the use of inert high surface silica nanoparticles with reactive chemicals could be the best way to remove and detoxify CW agents. Here, high surface area of silica can bring an increase in physisorption efficiency and loaded reactive chemicals can impart chemical degradation capability to the system for the degradation of adsorbed toxicants.

Reactive adsorbents can degrade CW agents by variety of reactions, such as oxidation, hydrolysis, elimination, addition and dealkylation [13]. In 2002, Narske et al. [14] performed the adsorptive removal of 2-CEES from pentane solution using AP-MgO. He indicated the formation of 2-HEES [(2-hydroxyethyl)ethyl sulphide] and ethylvinyl sulphide as reaction products. Wagner et al. have investigated room temperature destruction of actual CW agents such as GB (isopropylmethylphosphonofluoridate), bis-(2-chloroethyl)sulphide [(sulphur mustard, HD), a cytotoxic, alkylating vesicant CW agent], etc. on nanoparticles of magnesium oxide [2] and aluminum oxide [3] using solid-state MAS-NMR technique. He has indicated the half-life of degradation of HD over AP-Al_2O_3 and AP-MgO to be 6.3 h and 17.8 h, respectively. Moreover, study indicated that the hydrolysis and dehydrohalogenation of these agents took place on the surface of metal oxide nanocrystals and thereby, HD degraded to thiodiglycol, 2-chloroethylvinyl sulphide and divinyl sulphide.

Inspired by this, aerogel produced silica (AP-SiO_2) nanoparticles have been synthesized by aerogel process [15] and subsequently characterized. Thereafter, to increase their reactivity and give them a permanent self-decontaminating feature these have been impregnated with reactive chemicals using incipient wetness technique [6]. Later, these were explored to understand the adsorption kinetics of HD from solution [14] and find out the best system for the reactive removal of HD. The aim of the study was to develop indigenous sorbent system, which can be used in decontamination devices and filtration systems with suitable modifications (converting impregnated nanoparticles to granules by mechanical compression technique) to remove and detoxify CW agents effectively in less time.

2. Experimental

2.1. Synthesis of silicone oxide nanoparticles

AP-SiO_2 nanoparticles have been synthesized using "bottom-up" wet chemical method (aerogel process) and stoichiometric amount of reactants in toluene/methanol solvent system as given for the synthesis of AP-MgO [1]. For that 83.2 g of tetraethoxysilane was taken in a 1000-mL round-bottomed flask having 500 mL of ethanol. To this 500 mL of toluene was added and the solution was stirred for 30 min under an inert atmosphere of nitrogen gas. Thereafter, a solution of stoichiometric amount, i.e., 28.8 mL (1.6 M) of triple distilled and deionized water in 240 mL of ethanol and 735 mL of toluene was prepared. This solution was slowly added to the solution prepared in first step with vigorous stirring in 3.0 L round-bottomed flask. The solution was covered with aluminum foil and stirred for 4 h. This resulted into opaque liquid-like gel.

Next 600 mL of thus formed silicon hydroxide gel was transferred to 1000 mL capacity parr autoclave. The gel was first flushed with inert gas and the reaction was carried out under inert gas with an initial pressure of 100 psi. The reactor was slowly heated from room temperature to 265 °C at the rate of 1.0 °C/min and the time of heating was 4 h. After reaching the desired temperature (265 °C), the reactor was maintained at this temperature for 10 min. During heating the pressure inside the autoclave was increased to 800 psi. The system was quickly vented to the atmosphere for over a period of 1 min. The furnace was taken off and the produced powder was flushed with inert gas for 15 min to remove the remaining solvent vapours. The autoclave was allowed to cool to room temperature over approximately 3 h. After that produced material was thermally treated. For that, 25 g of thus produced powder was placed in 500 mL capacity thermal reactor. This was evacuated for 30 min at room temperature. Later, it was slowly heated for 6 h from room temperature to 500 °C under dynamic vacuum of 10^{-2} Torr and kept under this condition for 10 h. Finally, the material was cooled to room temperature under vacuum, flushed with inert gas and stored in air tight bottles till further use.

2.2. Loading of impregnants on silica nanoparticles

In order to prepare impregnated nanoparticles AP and CM-silica (commercially available silica particles) were impregnated (5–15%, w/w) with *N*-chloro compounds, oxaziridine and other reactive chemicals. *N*-chloro compounds used for impregnation were *N*,*N*′-dichloro-bis(2,4,6-trichlorophenyl) urea (CC-2), trichloroisocyanuric acid (TCCUA), *N*-*tert*-butyl-*N*-chlorocyanamide (NTBNCC), chloramine-T dichloramine-T (DCT), *N*-chloro saccharin (NCS) and 2,4-dichlorophenyl benzoylchloroimide (SDR). Other reactive chemicals loaded on nanosilica particles were *N*-methyl morpholin-4-oxide (NMMO), benzoyl peroxide (BPO), ruthenium trichloride, 3-chloroperbenzoic acid (CPBA), sodium hydroxide, 2,4-dichlorophenyl benzoylchloroimide (1*R*)-(−)-(camphorylsulphonyl) oxaziridine, 9-molybdo-3-vanadophosphoric acid [MoVPA (V_3)]: $H_6[PMo_9V_3O_{40}]\cdot 34H_2O$ and Dodeca tungstophosphoric acid (PTA): $H_3PW_{12}O_{40} \times H_2O$. Impregnants in aqueous or organic solvent (corresponding to incipient volume of silica nanoparticles, i.e., 1 mL/100 mg silica) were used for impregnation and the technique used for this was incipient wetness technique [6]. For impregnation the solution of oxaziridine and CC-2 in dichloromethane; DCT, NTBNCC and SDR in carbon tetrachloride; TCCUA in acetone; NCS in acetonitrile, BPO and CPBA in benzene; other impregnants in water were prepared. Thereafter, the appropriate solution was poured to the beaker having silica nanoparticles and mixed vigorously. Thus prepared material was dried at 110 °C for 4 h, cooled in desiccators under dried calcium chloride and finally stored in airtight bottles till further use.

Gas phase CW agent decontamination devices may use the nanoparticles powder as such, while filtration systems shall require granulled nanoparticles-based material. For that 50–200 mg pellets with the density of 0.1–0.3 g/cm^3 were prepared using manual pelletting machine by applying a pressure of 5.0–15 $\times$ 10^5 N/m^2. These pellets of different sizes [3–8 mm diameter and 5–15 mm height (Fig. 1)] were made. These pellets were also broken down to granules of different sizes (Fig. 1). Thus produced metal oxide granules and pellets represent a new family of porous inorganic materials where pore structure can also be roughly controlled by compression technique.

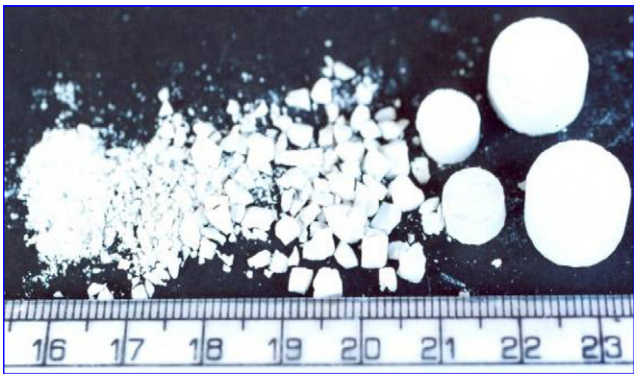

Fig. 1. AP-SiO_2 nanoparticles-based material in the shape of pellets, granules and powder.

2.3. Characterization of silica nanoparticles-based adsorbents

Prior to use, silica nanoparticles with and without impregnants were characterized for porosity and surface characteristics using various techniques such as surface area analysis, scanning electron microscopy, transmission electron microscopy, etc. The material was also characterized for acid/base neutralization capacity, bulk density and moisture content.

2.4. Surface area and porosity

Surface area and pore size distribution of AP and CM-SiO_2 with and without impregnants were determined using Autosorb-1-C from Quantachrome, USA. The samples were first outgassed under dynamic vacuum (10^{-2} Torr) for 8 h at 200 °C and then allowed to cool to room temperature. After that, the N_2 adsorption–desorption isotherms were obtained at liquid nitrogen temperature, i.e., 77 K. Surface area and micro pore volume were determined using Brunauer–Emmet–Teller (BET) and Dubinin–Radushkevich (DR) methods, respectively. Cumulative desorption pore volume was determined using Barrett–Joyner–Halenda (BJH) method. Pore maxima for micropores (<2 nm) and mesopores (2–50 nm) were determined considering BJH and DFT (density functional theory) methods. The surface area, micropore volume, cumulative desorption pore volume and pore maxima for micropores and mesopores

Table 1
Surface area and poresize distribution of silica with and without oxaziridine impregnation, and kinetics parameters for the removal of HD

Metal oxide system + percentage impregnation of oxaziridine (w/w)	Surface area (N_2 BET) (m^2/g)	Micropore volume (N_2 DR) (cm^3/g)	Cumulative desorption pore volume (N_2 BJH) (cm^3/g)	Pore maxima for micropores and mesopores (Å)		Half-life (min)	Rate constant ($\times 10^{-3}$ min^{-1})
				Micro	Meso		
AP-SiO_2 + nil	887.3	0.386	1.451	14.6	27.5	1210	0.57
CM-SiO_2 + nil	389.2	0.178	0.696	11.6	41.7	1180	0.58
AP-SiO_2 + 5%	630.7	0.267	0.688	14.6	25.5	32	21.66
CM-SiO_2 + 5%	342.8	0.155	0.588	11.6	41.8	302	2.29
AP-SiO_2 + 10%	582.0	0.251	0.669	14.8	25.2	14	49.50
CM-SiO_2 + 10%	320.8	0.140	0.565	11.6	41.8	15	46.20
AP-SiO_2 + 15%	508.2	0.238	0.654	14.8	24.8	12	57.75
CM-SiO_2 + 15%	300.6	0.131	0.554	11.4	41.0	10	69.30

Table 2
Surface area and poresize distribution of *N*-chloro compounds impregnated silica nanoparticles, and kinetics parameters for the removal of HD

Metal oxidesystem + impregnation (10%, w/w)	Surface area(N_2 BET) (m^2/g)	Micropore volume (N_2 DR) (cm^3/g)	Cumulative desorption pore volume (N_2 BJH) (cm^3/g)	Pore maxima for micropores and mesopores (Å)		Half-life (min)	Rate constant ($\times 10^{-3}$ min^{-1})
				Micro	Meso		
AP-SiO_2 + TCCUA	682.9	0.302	0.839	15.1	24.5	2.8	247.5
AP-SiO_2 + DCT	672.2	0.300	0.823	15.1	24.6	3.1	223.5
AP-SiO_2 + NTBNCC	500.4	0.268	0.713	14.8	24.8	32.0	21.6
AP-SiO_2 + CC2	702.2	0.323	0.868	15.1	24.6	410.0	1.69
AP-SiO_2 + NCS	590.7	0.293	0.810	15.4	24.8	680.0	1.02
AP-SiO_2 + SDR	678.3	0.304	0.832	15.3	24.8	870.0	0.80

Table 3
Surface area and poresize distribution of impregnated silica systems, and kinetics parameters for the removal of HD

Metal oxide system + impregnation (10%, w/w)	Surface area (N_2 BET) (m^2/g)	Micropore volume (N_2 DR) (cm^3/g)	Cumulative desorption pore volume (N_2 BJH) (cm^3/g)	Pore maxima for micropores and mesopores (Å)		Half-life (min)	Rate constant ($\times 10^{-3}$ min^{-1})
				Micro	Meso		
AP-SiO_2 + $RuCl_3$	625.1	0.282	0.679	14.9	27.2	150.0	4.62
AP-SiO_2 + PTA	624.5	0.288	0.670	14.8	27.0	338.0	2.05
AP-SiO_2 + BPO	680.8	0.298	0.698	14.5	27.2	611.0	1.13
AP-SiO_2 + CPBA	580.2	0.265	0.635	14.5	27.0	620.0	1.12
AP-SiO_2 + $KHSO_5$	438.8	0.214	0.571	14.9	27.2	720.0	0.96
AP-SiO_2 + NMMO	500.2	0.256	0.634	14.8	27.2	840.0	0.83
AP-SiO_2 + NaOH	120.6	0.049	0.166	15.1	27.5	1320.0	0.53
AP-SiO_2 + MoVPA (V_3)	615.4	0.280	0.672	14.5	27.1	310.0	2.24
CM-SiO_2 + MoVPA (V_3)	328.8	0.143	0.343	14.5	27.2	790.0	0.88
AP-SiO_2 + K_2OsO_4	788.3	0.326	0.868	15.2	27.2	501.0	1.38
CM-SiO_2 + K_2OsO_4	334.0	0.164	0.388	14.6	27.1	870.0	0.79

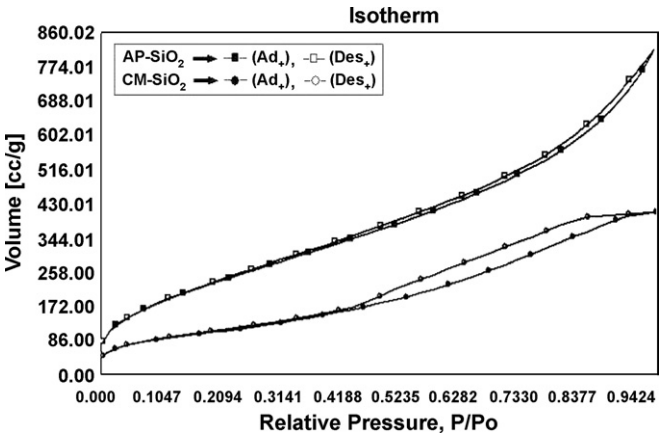

Fig. 2. Adsorption isotherms of AP-SiO_2 and CM-SiO_2.

have been presented in Tables 1–3. Figs. 2 and 3 describe the nitrogen adsorption–desorption isotherms and pore size distributions of AP and CM-SiO_2.

2.5. Scanning electron microscopy, transmission electron microscopy and X-ray diffraction studies

For SEM characterization, the powder samples were first mounted on brass stubs using double-sided adhesive tape and then gold coated for 8 min using ion sputter JEOL, JFC 1100 coating unit. The surface texture of silica nanoparticles was observed using FEI ESEM Quanta 400. Fig. 4 represents the SEM image. TEM studies were performed to find out the particle size of the synthesized materials. For that 10 mg of sample was mixed in 10 mL of pentane and sonicated for 2 h to achieve a better separation of the particles. A drop of supernatant of the solution was placed on the copper grid of 200 mesh size followed by carbon coating. TEM images were recorded using JEOL, JEM-1200 Ex. For XRD studies the powder samples were heat treated under vacuum before placing onto the sample holder. The instrument used was Philips XRD PW 3020. Cu Kα radiation ($\lambda = 0.154$ nm) was the light source used with applied voltage of 40 KV and current of 40 mA. The 2θ angles ranged from 20° to 80° with a speed of 0.05°/s. The crystallite size was then calculated from the XRD spectra using Scherrer equation. Figs. 5 and 6 show the TEM image and XRD pattern of AP-SiO_2, respectively. Fig. 7 shows the TEM image of AP-SiO_2 + TCCUA system.

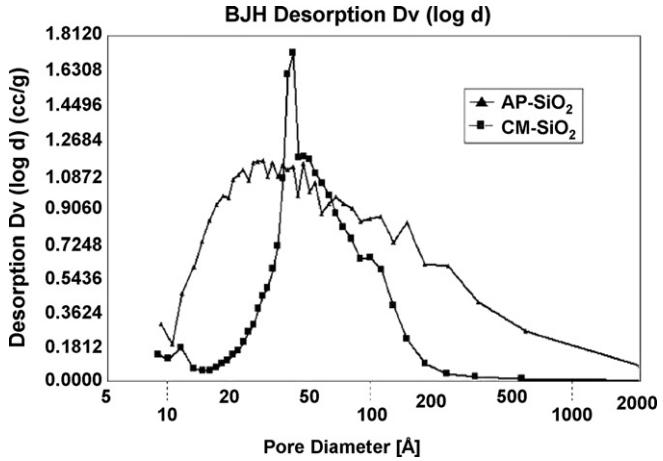

Fig. 3. BJH pore size distributions of AP-SiO_2 and CM-SiO_2.

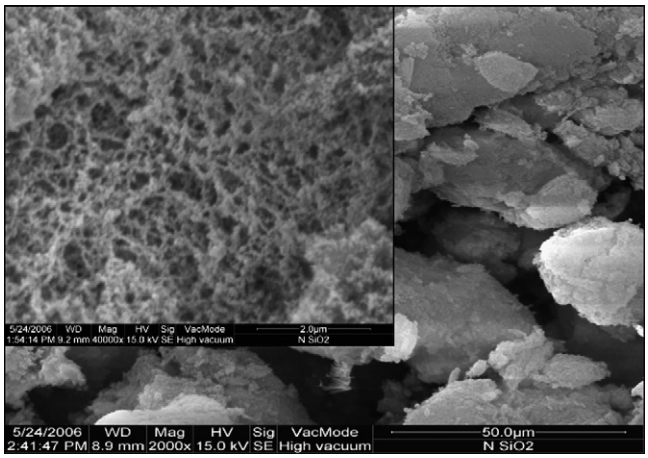

Fig. 4. SEM image of AP-SiO_2.

2.6. Acid/base neutralization capacity, bulk density and moisture content

In order to find out acid/base neutralization capacity of AP and CM-SiO_2, 20 mg of sample was taken in 20 mL of triple distilled and deionized water and stirred for 10 min. The pH of the solution was continuously noted. Then it was titrated with 0.01N HCl/NaOH till the pH of the solution reached to 6.5 (initial value of pH of distilled water). The bulk density of synthesized and commercial materials were measured by weighing a known volume (20 mL) of material and expressed in g/mL. The moisture content of the material was determined by heating a known amount (1 g) of sample in oven at 120 °C for 6 h, cooling in desiccators for 1 h and finally weighing. The weight loss in sample per 100 g was taken as moisture content of the material.

2.7. Kinetics of reactive removal of HD

In order to study the kinetics of removal of HD at room temperature (25 ± 1 °C) 2.5 μL of HD was mixed with 4 mL of octane in glass vials (8 mL capacity with Teflon septum caps). Octane was

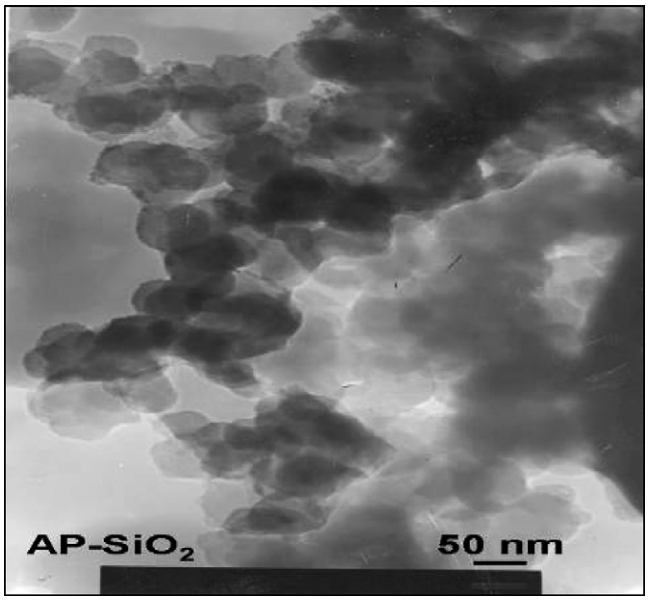

Fig. 5. TEM image of AP-SiO_2.

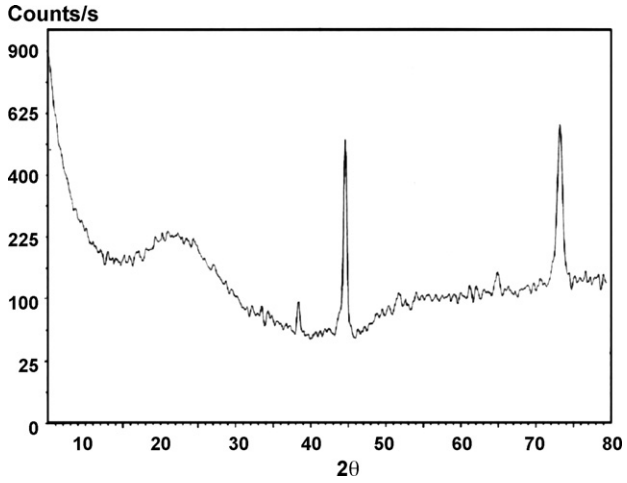

Fig. 6. XRD pattern of AP-SiO_2.

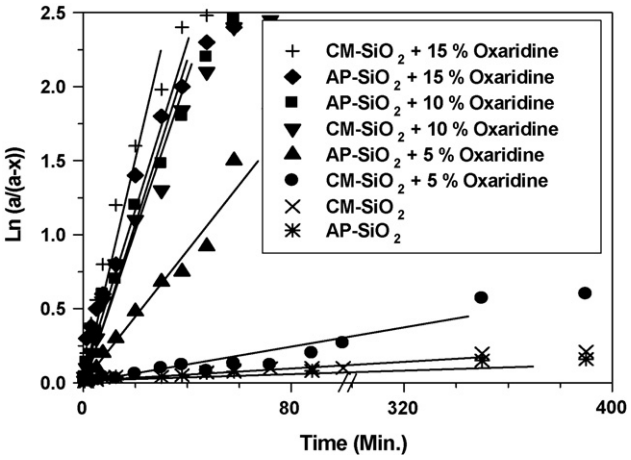

Fig. 8. Kinetics of removal of HD on oxaziridine (5%, 10% and 15%) impregnated AP and CM-silica particles.

chosen as a solvent for the current work due to the inertness of it against reactive impregnants with respect to solubility and reactivity, and this also decreases the possibility of leaching of reactive impregnant in octane solution. After that 50 mg of prepared silica nanoparticles (with and without impregnation) was suspended to the solution and the vials were capped. These were continuously rotated at the speed of 50 rpm using Tarsons Rotospin. After definite time intervals 1 μL of the solution was taken out from glass vials and analyzed for residual amount of toxicant using GC/FID. Results were compared against the control experiment without systems under the same experimental conditions. Figs. 8–10 represent the kinetics of removal of toxicants and Tables 1–3 show the half-life and rate constant values.

In order to study the kinetics of degradation or adsorptive removal of toxicants on metal oxide nanoparticles with and without impregnants, $\mathrm{Ln}[a/(a-x)]$ (where "a" is the initial amount and "$(a-x)$" is the remaining amount of toxicant at time, t) on Y-axis was plotted against reaction time, t on X-axis. Rate constant (K) was calculated using the slope of the straight line and half-life ($t_{1/2}$) by $0.693\,K^{-1}$.

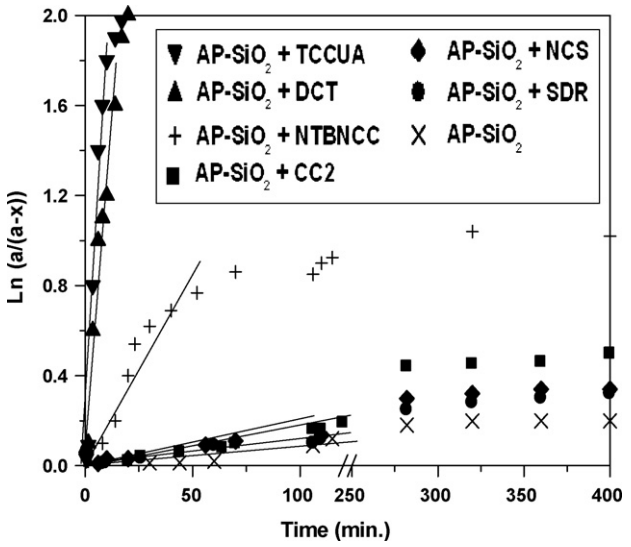

Fig. 9. Kinetics of removal of HD on AP-SiO_2 nanoparticles impregnated with *N*-chloro compounds.

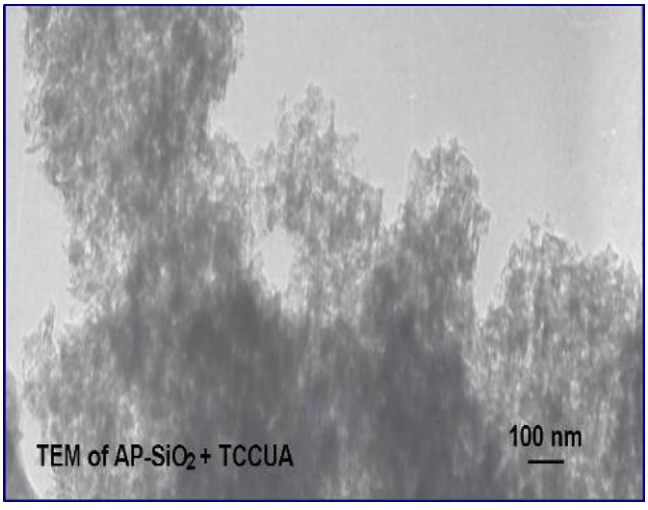

Fig. 7. TEM image of AP-SiO_2 + TCCUA system.

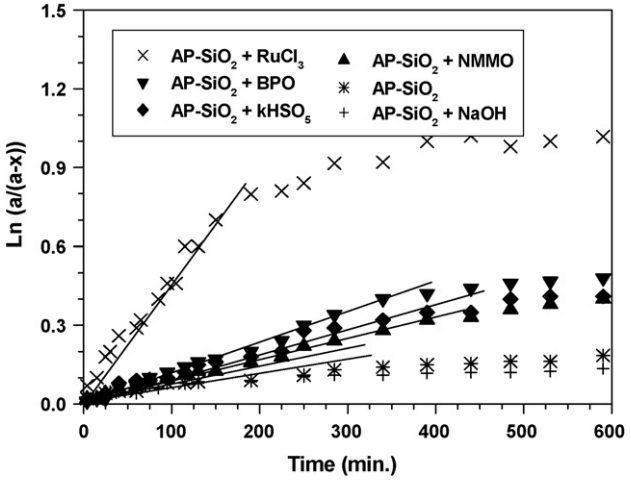

Fig. 10. Kinetics of removal of HD on impregnated AP-SiO_2 nanoparticles.

2.8. Identification of reaction products

In order to investigate the reaction products 10 mg of toxicant exposed nanoparticle-based adsorbents were extracted with 2.0 mL of acetonitrile for 2 h in a well-stoppered test tube. The extracts were centrifuged and transferred to another tube. The extracts were then purged with nitrogen gas to concentrate the extracted reaction products and subjected to product identification using GC/MS (gas chromatograph coupled with mass spectrometer) instrumental techniques. GC/MS (6890N GC coupled with 5973 inert MS detector) of Agilent Technologies, USA was used for characterization of reaction products. It was equipped with HP-5MS column of 30 m × 0.25 mm × 0.25 μm dimensions. Temperature programming [50 °C (2 min hold) to 280 °C (10 min hold) at 10 °C/min] with split injection technique (10:1) was used to perform the study. Injection port and GC/MS interface, MS source and quadrupole analyzer were kept at 280 °C, 230 °C and 150 °C, respectively.

3. Results and discussion

3.1. Characterization of silica nanoparticles-based adsorbents

Figs. 2 and 3 represent the nitrogen adsorption–desorption isotherms and BJH pore size distributions, respectively for AP and CM-SiO_2 nanoparticles. AP-SiO_2 showed highest uptake of nitrogen and exhibited hysteresis loop, which is the characteristic of adsorption possessing a portion of mesopores with mesopore maxima at 27.5 Å (Fig. 2 and Table 1). Apart from mesoporous characteristics AP-SiO_2 was also found to be having micropores with micropore maxima at 14.6 Å. The surface area of AP-SiO_2 was found to be 887.3 m^2/g, which was more than double of its counterpart, i.e., CM-SiO_2 (surface area = 389.2 m^2/g). BJH cumulative desorption pore volume for AP-SiO_2 was also more than double of CM-SiO_2. Micropore and cumulative desorption pore volume of AP-SiO_2 were found to be 0.386 cm^3/g and 1.451 cm^3/g, respectively.

Tables 1–3 represent the surface area, bulk density and moisture content of all impregnated AP and CM-SiO_2-based adsorbent systems with and without impregnants. AP-SiO_2 when was impregnated with oxaziridine [5%, w/w], surface area decreased from 887.3 m^2/g to 630.7 m^2/g (Table 1). This decrease was due to impregnants, which during impregnation travel through the macropores and gets deposited in the mesopores or the pore opening of micro pores to cause the blocking of the meso/micropores [6]. Decrease in surface area after impregnation was found with all samples, whether synthesized nanoparticles or commercial metal oxides (Tables 1–3). AP-SiO_2 with NaOH impregnations (10%, w/w) showed maximum reduction in surface area, i.e., from 887.3 m^2/g to 120.6 m^2/g. This was probably due to the reaction of SiO_2 with NaOH to result sodium silicate. All silica samples showed strong mesoporous characteristics. Apart from mesoporous characteristic they were also found to be having micropores. In addition to this, all nanosilica samples showed the same type of pore size distributions with micropore and mesopore maxima at ∼15 Å and ∼25 Å, respectively. Micropore (N_2-DR) and cumulative desorption pore volume (N_2-BJH) of AP-SiO_2 were also found to be decreased after impregnation.

Fig. 4 represents the SEM image of AP-SiO_2. The image clearly indicated the web/net like structure of nanoparticle aggregates with a quantum of huge porosity, which is confirmed by its surface area value (887.3 m^2/g). TEM image of AP-SiO_2 (Fig. 5) indicated the particles to be in the size range of 24–75 nm with maximum particles in the range of 30–40 nm. Moreover, 25 nm diameter particles weakly agglomerate into a mass with large pores, where the pores are actually the space between the particles (as opposed to holes and channels in the particles themselves). Fig. 6 shows the XRD pattern of amorphous AP-SiO_2 with particle diameter of 12–24 nm (determined using Scherrer equation). These particles, when impregnated with TCCUA the particle size changed to 38–90 nm (Fig. 7) with maximum particles in the range of 45–55 nm.

AP and CM-SiO_2 indicated slightly surface acidity, which was equivalent to 3.3 mmol and 1.5 mmol of NaOH per mole of silica, respectively. The bulk density of AP-SiO_2 was found to be ∼1/16th (0.035 g/mL) of its counterpart, i.e., CM-SiO_2 (0.573 g/mL). For impregnated systems it was found to be in the range of 0.046 g/mL (AP-SiO_2 + oxaziridine) to 0.102 g/mL (AP-SiO_2 + NaOH). Moreover, all AP and CM-SiO_2-based samples indicated the increase in bulk densities after impregnation due to the reason that during impregnation impregnants sit in the mesopores of adsorbent, i.e., the weight increases, whereas the outer surface volume of the material remains same, hence density increases. A threefold increase (from 0.035 g/mL to 0.102 g/mL) in bulk density of AP-SiO_2 + NaOH system has also indicated the reaction of SiO_2 with NaOH as that of indicated by decrease in surface area values (Tables 1 and 3). Moisture content of all prepared systems was found to be in the range of 0.8–3.1% (w/w).

3.2. Kinetics of reactive removal of HD

Figs. 8–10 represent the kinetics of reactive removal of HD on silica nanoparticles-based systems with and without impregnants. Tables 1–3 represent the half-life and rate constant values. These figures clearly indicated that the adsorption kinetics is initially fast, which gradually slowed down to a steady state kinetics at later intervals of time [2,3]. This can be understood by having an insight in the adsorption process, which includes physisorption and chemisorption of HD. As the prepared silica nanoparticles-based systems are added to the solution of HD in octane, the physisorption of HD starts, i.e., the HD molecules approach to the physisorption sites and get physisorbed. Progressively the number of sites decreases due to physisorption of HD and due to this the physisorption slows down and ends to a steady state. The physisorption efficiency of adsorbents mainly depends on surface area, higher the surface area higher will be the adsorption potential. Apart from surface area, the adsorption potential also depends on pore size distribution of adsorbent and molecular diameter and nature of adsorbate. In present study the adsorbate (HD) remains same, whereas the adsorbent systems are different; hence the adsorption potential should depend on surface area and porosity of different adsorbents. The characterization of the adsorbents indicated that all silica nanoparticles-based systems have the same type of pore size distributions with micropore and mesopore maxima at ∼15 Å and ∼25 Å, respectively; hence the adsorption potential for the present study should depend on surface area values of adsorbents. But, if first two entries of Table 1 are compared, then the $t_{1/2}$ values clearly indicated that CM-SiO_2 has lesser surface area than AP-SiO_2, but indicated higher adsorption potential, i.e., lesser $t_{1/2}$ value. Similarly, if AP-SiO_2 has been impregnated with 15% oxaziridine (Table 1 entry 3) the $t_{1/2}$ decreased sharply from 1210 min to 12 min. This again indicated that the adsorption kinetics also depends on chemisorption/degradation of HD. Moreover, this indicated that as the HD molecule is physisorbed on impregnated silica nanoparticles, it starts reacting with the active sites of adsorbent or the impregnants available on their surface, and thereby leading to the destruction of HD molecules to nontoxic products. This results in a sharp decrease of $t_{1/2}$ values. In order to further check, whether HD is physisorbed or chemisorbed/degraded on nanoparticles-based systems 2 mL of acetone (polar solvent) was added to the reaction

mixture after kinetics study. The reaction mixture was stirred for 5 min and then subjected to GC/FID. Study indicated the results to be ±5.0% as that of obtained with kinetics of removal study (HD in octane). Therefore, the study indicated that the destructive adsorption of HD takes place on impregnated silica nanoparticles, thus giving a self-decontaminating feature to the adsorbent systems.

Fig. 8 represents the effect of percentage of impregnation of oxaziridine on adsorptive removal kinetics for sulphur mustard. AP and CM-SiO_2 without impregnation showed the slowest kinetics, whereas the rate of kinetics increased due to the presence of oxaziridine (5–15%). Due to 15% oxaziridine impregnation, the increase in rate constant was found to be from 0.57×10^{-3} min^{-1} to 57.75×10^{-3} min^{-1}. Fig. 8 and Table 1 clearly indicated that an increase in percentage of impregnation increases the rate of kinetics of removal. But an increase in percentage of impregnation from 10 to 15 did not result in much difference. It could reduce the $t_{1/2}$ from 14 min to 12 min with silica nanoparticles. With 15% oxaziridine CM-SiO_2 showed better results than AP-SiO_2, whereas 5–10% oxaziridine impregnation indicated AP-SiO_2 to be better than CM-SiO_2. As the difference in $t_{1/2}$ values for 10–15% oxaziridine impregnation on AP/CM-SiO_2 was not much (Table 1) or it was within the experimental precision, therefore, no firm conclusion could be made. Moreover, the study indicated that impregnation of reactive chemicals (10%, w/w) over silica nanoparticles is sufficient enough to achieve loading effect for the reactive removal of HD. In addition to that, impregnation of silica nanoparticles with oxaziridine resulted in the decrease in surface area values (10–30%), whereas the kinetics of removal was found to be reversed. This clearly highlighted that the kinetics of removal of HD was independent of surface area of oxaziridine impregnated systems.

Fig. 9 shows the kinetics of removal of HD on AP-SiO_2 impregnated with reactive *N*-chloro compounds (10%, w/w) and the results have been tabulated in Table 2. AP-SiO_2 + TCCUA system showed outstanding performance with lowest $t_{1/2}$ value, i.e., 2.8 min, this was even lower than all oxaziridine impregnated systems (Table 1). AP-SiO_2 + TCCUA system also indicated > 90% HD removal within 15 min, whereas ~100% in 25 min. When HD was allowed to react with similar amount of TCCUA as with (AP-SiO_2 + TCCUA) system in octane, the reactions were stoichiometric and fast. For TCCUA, $t_{1/2}$ was <1 min against 2.8 min with impregnated system [AP-SiO_2 + 10% TCCUA (w/w)]. CC-2 [9], which is an efficient chlorine releasing reagent and has been incorporated as a reactive ingredient in a formulations developed to decontaminate HD showed higher $t_{1/2}$ value than TCCUA impregnated silica nanoparticles. Dichloramine-T impregnated AP-SiO_2 also showed promising results with $t_{1/2}$ of 3.1 min. Dubey et al. [10] have also indicated dichloramine-T as an excellent decontaminant against mustard, especially in situations where use of aqueous medium is precluded. Overall, *N*-chloro compounds impregnated silica nanoparticles-based systems showed the following order for reactive removal efficiency against HD: AP-SiO_2 + TCCUA > AP-SiO_2 + DCT > AP-SiO_2 + NTBNCC > AP-SiO_2 + CC2 > AP-SiO_2 + NCS > AP-SiO_2 + SDR.

Among oxidizing agents and other reactive chemicals impregnated AP-SiO_2 systems (Fig. 10, Table 3), AP-SiO_2 + $RuCl_3$ system showed best results ($t_{1/2}$ = 150 min). NaOH impregnated AP-SiO_2 systems showed even less activity than unimpregnated nanoparticles. This was due to the reaction of NaOH with silica nanoparticles to make sodium silicate. MoVPA (V_3) and PTA impregnation to silica nanoparticles also indicated good results with $t_{1/2}$ values of 310 min and 338 min, respectively. MoVPA (V_3) and K_2OsO_4 impregnation to silica nanoparticles also indicated the suitability of nanoparticles over commercial silica. Moreover, impregnation of BPO, CPBA, $KHSO_5$, NMMO, NaOH and K_2OsO_4 over silica nanoparticles could not show promising results, hence indicated the unsuitability of them to use with silica nanoparticles for the reactive removal of HD.

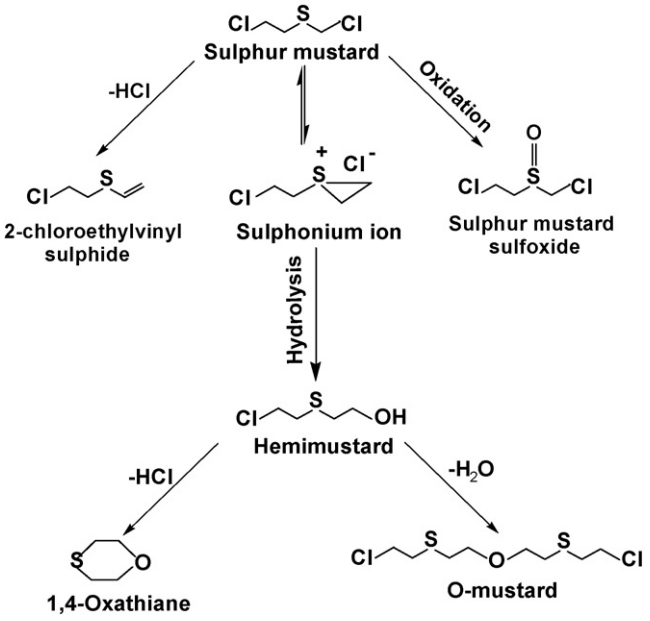

Scheme 1.

3.3. Identification of reaction products

The study on kinetics of adsorptive removal of HD indicated that HD molecules interact instantaneously with the impregnants available on silica and thereby made nontoxic due to the conversion of HD to nontoxic degradation products. In order to find out reaction products these either have to be investigated directly using MAS-NMR technique [2,3] or by extracting them in organic solvent and analyzing through GC/MS [16]. Moreover, in the present study reaction products have been identified using GC/MS analysis of extracts. The mass spectra of reaction products have been compared with the standard mass spectra from existing libraries (Wiley and NIST) of GC/MS instrument.

AP-SiO_2 indicated the formation of 2-chloroethylvinyl sulphide only as a reaction product of HD. When AP-SiO_2 was impregnated with trichloroisocyanuric acid (AP-SiO_2 + TCCUA), the system indicated that HD undergoes hydrolysis reaction with the formation of intermediate sulphonium ion [17]. Sulphonium ion is formed due to the attack of sulphide on the β carbon atom of HD and is considered to be SN^1 reaction. Sulphonium ion is highly unstable, because of which it could not be extracted and detected. Subsequently, the sulphonium ion undergoes hydrolysis with the water available with nanoparticles under study (no more water is added prior to the reaction) and gives rise to the formation of hemimustard (Scheme 1). Apart from hydrolysis, dehydrohalogenation reaction was also found to be occurring as a mode of degradation of HD. Wagner et al. [2,3] have also indicated the hydrolysis and dehydrohalogenation reactions of HD on nanocrystalline metal oxides. Overall, hemimustard (*m*/*z* values at 140, 109, 91 and 63, a hydrolysis reaction product of HD), chloroethylvinyl sulphide (via dehydrohalogenation reaction), 1,4-oxathiane and O-mustard($Cl–CH_2–CH_2–S–CH_2–CH_2–O–CH_2–CH_2–S–CH_2–CH_2–Cl$) were observed as reaction products of HD. O-mustard is probably formed via the combination of two hemimustard molecules with the removal of water. In addition to these products oxaziridine, polyoxometalates and $RuCl_3$ impregnated silica nanoparticles indicated the formation of HD-sulphoxide, an oxidation product of

HD. The formation of oxidation product was due to the presence of impregnants ($RuCl_3$, polyoxometalate and oxaziridine), which have already been known for oxidation reactions [9,18,19].

4. Conclusion

AP-SiO_2 nanoparticles with high surface area and particle diameter in the range of 24–75 nm were synthesized using aerogel route. These were impregnated with reactive chemicals and subsequently characterized for porosity and surface morphology. All nanosilica samples showed the same type of pore size distributions with micropore and mesopore maxima at ~15 Å and ~25 Å, respectively. Thereafter, studies on kinetics of reactive removal of HD on prepared systems were performed. AP and CM-SiO_2 without impregnation showed the slowest kinetics, whereas the rate of kinetics increased due to the presence of oxaziridine (5–15%). Impregnation of oxaziridine (15%, w/w) on silica nanoparticles reduced the $t_{1/2}$ value from 1210 min to 12 min (reduction by 100 times). AP-SiO_2 + TCCUA system showed highest adsorption potential with highest rate constant (247.5×10^{-3} min^{-1}) among all studied silica nanoparticles-based systems against HD. Moreover, impregnated silica nanoparticles-based systems indicated that the reactive removal of HD was not only due to physisorption but also involved chemisorption, where the physisorbed toxicant molecules diffuse to the chemisorption sites and react with the impregnants, ultimately resulting in the increased adsorption potential.

AP-SiO_2 + TCCUA system indicated the formation of 2-chloroethylvinyl sulphide, 1,4-oxathiane, hemimustard and O-mustard as reaction products of HD. In association to this oxaziridine and $RuCl_3$ impregnated silica nanoparticles indicated the formation of HD-sulphoxide. Overall, it is inferred from the study that AP-SiO_2 + TCCUA system can promisingly be used in gas phase chemical warfare agent removal/decontamination devices and NBC filtration systems. In addition to this, the study also concluded that the impregnation of reactive chemicals or catalysts (10%, w/w) over silica nanoparticles is appropriate to get promising loading effect and the same can be utilized for different type of reactions in the field of catalysis, chemical conversions, decontamination of toxic chemicals, etc.

Acknowledgements

We thank Dr. R. Vijayaraghavan, Director, DRDE, Gwalior, for providing lab facilities to carry out and publish this work. We also thank Dr. M.V.S. Suryanarayana, Dr. R.P. Semwal and Dr. P. Pandey for useful suggestions.

References

[1] K.J. Klabunde, Nanoscale Materials in Chemistry, John Wiley and Sons, New York, 2001.
[2] G.W. Wagner, P.W. Bartram, O. Koper, K.J. Klabunde, Reactions of VX, GD, and HD with nanosize MgO, J. Phys. Chem. B 103 (1999) 3225–3228.
[3] G.W. Wagner, L.R. Procell, R.J. O'Corner, S. Munavalli, C.L. Carnes, P.N. Kapoor, K.J. Klabunde, Reactions of VX, GB, GD, and HD with nanosize Al_2O_3-formation of aluminophosphonates, J. Am. Chem. Soc. 123 (2001) 1636–1644.
[4] O. Koper, K.J. Klabunde, Reactive nanoparticles as destructive adsorbents for biological and chemical contamination, US Patent WO 01/78506 A1 (2001).
[5] G.K. Prasad, B. Singh, A. Saxena, Kinetics of adsorption of sulfur mustard vapors on carbons under static conditions, AIChE J. 52 (2) (2006) 678–682.
[6] A. Saxena, B. Singh, A. Sharma, V. Dubey, R.P. Semwal, M.V.S. Suryanarayana, V.K. Rao, K. Sekhar, Adsorption of dimethylmethylphosphonate on metal impregnated carbons under static conditions, J. Hazard. Mater. 134 (1–3) (2006) 104–111.
[7] J.G. Purdon, C.L. Chenier, A.F.H. Burczyk, Broad spectrum decontamination formulation and method of use, US Patent 6,525,237 (2003).
[8] F.A. Davis, S.M. Haque, Oxygen transfer reaction of oxaziridines, in: A.L. Baumstark (Ed.), Advances in Oxygenated Processes, J.A.L. Press, Greenwich, CT, 1990.
[9] B.C. Bag, K. Sekhar, D.K. Dubey, M. Sai, R.S. Dangi, M.P. Kaushik, C. Bhattacharya, An effective process for conversion of diphenylurea to CC-2, a potential decontaminant of sulfur mustard, Org. Process Res. Dev. 10 (3) (2006) 505–511.
[10] D.K. Dubey, R. Nath, R.C. Malhotra, D.N. Tripathi, Degradation of 2,2′-dihalodiethyl sulfides(mustards) by *N*,*N*-dichloro-4-methylbenzenesulphonamide in aprotic medium, Tetrahedron Lett. 34 (47) (1993) 7645–7648.
[11] N. Okun, C.L. Hill, Materials for degrading contaminants, US Patent WO 03/094977 A2 (2003).
[12] H. Lomasney, C. Lomasney, J. Grawe, Chemically and/or biologically reactive compounds, US Patent WO 03/092656 A1 (2003).
[13] J.G. Ekerdt, K.J. Klabunde, J.R. Shapley, J.M. White, J.T. Yates Jr., Surface chemistry of organophosphorus compounds, J. Phys. Chem. 92 (1988) 6182–6188.
[14] R.M. Narske, K.J. Klabunde, S. Fultz, Solvent effects on the heterogenous adsorption and reactions of (2-chloroethyl)ethyl sulphide on nanocrystalline magnesium oxide, Langmuir 18 (2002) 4819–4825.
[15] O.B. Koper, I. Lagadic, A. Volodin, K.J. Klabunde, Alkaline earth oxide nanoparticles obtained by aerogel methods—characterization and rational for unexpectedly high surface chemical reactivities, Chem. Mater. 9 (1997) 2468–2480.
[16] G.K. Prasad, T.H. Mahato, P. Pandey, B. Singh, M.V.S. Suryanarayana, A. Saxena, K. Sekhar, Reactive sorbent based on manganese oxide nanotubes and nanosheets for the decontamination of 2-chloroethylethyl sulphide, Micropor. Mesopor. Mater. 106 (2007) 256–261.
[17] P.D. Bartlett, C.G. Swain, Kinetics of hydrolysis and displacement reactions of *b*,*b*′-dichlorodiethyl sulfide (mustard gas) and of *b*-chloro-*b*-hydroxydiethyl sulfide (mustard chlorohydrin), J. Am. Chem. Soc. 71 (1949) 1406–1415.
[18] A. Sharma, A. Saxena, B. Singh, M. Sharma, M.V.S. Suryanarayana, R.P. Semwal, K. Ganeshan, K. Sekhar, In situ degradation of sulphur mustard and its simulants on the surface of impregnated carbon systems, J. Hazard. Mater. 133 (1–3) (2006) 106–112.
[19] R.P. Johnson, C.L. Hill, Polyoxometalate oxidation of chemical warfare agent simulants in fluorinated media, J. Appl. Toxicol. 19 (1999) S71–S75.